SPEED BRAKE BASED AIRSPEED CONTROL LAWS FOR CIVIL HIGH PRECISION FLIGHT MANEUVERS

H. Wilke*, P. Weber†, F. J. Silvestre *

* Technische Universität Berlin, Fachgebiet für Flugmechanik, Flugreglung & Aeroelastizität, Berlin, Germany
† Deutsches Zentrum für Luft- und Raumfahrt, Institut für Flugsystemtechnik, Manching, Germany

Abstract

Due to the inertia of jet engines, precise manual airspeed control is a demanding task. Accurate airspeed control is absolutely inevitable during air-to-air refuelling due to the close proximity of two aircrafts. In manual flight, the pilot's workload may increase considerably, and could be well reduced by the use of automatic flight control. In that case, due to their fast aerodynamic reaction in producing drag and directly affecting the airspeed, speed brakes have a potential improve the performance of automatic airspeed control functions for this mission type. The object of the paper is to propose two flight control law designs that automatically incorporate the speed brakes in the airspeed control law to reduce the pilot workload in high precision maneuvers. This is done by utilizing the fast dynamics of the speed brake to eliminate or compensate for the engine lag. The two control laws are implemented and compared in the paper by means of flight simulator tests. The results indicate a improvement of the handling qualities.

Keywords

Flight Control; Airspeed Control; Aerial Refuelling

NOMENCLATURE

Symbols

δ_{SB}	speed brake deflection	deg
γ	path angle	deg
δ_{thr}	thrust command	%
c_m	pitch moment coefficient	
c_x	force coefficient in x	
c_z	force coefficient in z	
d	distance	m
$e_{h,\mathrm{avg}}$	time-averaged altitude error	m
G	transfer function	
g	gravitational acceleration	m/s^2
h	altitude	m
K_p	(proportional) controller gain	
n_x	forward load factor	
r_{dr}	drogue radius	m
t_{cap}	capture time	s
t_e	end time	s
T_1	time constant	s
t_s	start time	s
V	airspeed	m/s
V_K	total velocity	m/s
V_{OT}	overtake speed	m/s
V_{ref}	reference airspeed	m/s
y_{dr}	lateral drogue position	m
y_{pr}	lateral probe position	m
z_{dr}	vertical drogue position	m
z_{pr}	vertical probe position	m

Indices

act	actuator
cmd	commanded
ctrl	(closed-loop) controller
eng	engine
HPF	high-pass filter
init	initial
LPF	low-pass filter
max	maximum
req	required

Abbreviations

AAR	air-to-air refuelling
CHR	Cooper-Harper-Rating
CPI	contact precision index
CSR	contact success rate
FFC	feed forward (control law)
HUD	head up display
PDR	probe-drogue-refuelling
SB	speed brake
SD	standard deviation
SEP	specific excess power

1. INTRODUCTION

Air-to-air-Refuelling (AAR) describes the process of transferring fuel from one aircraft (tanker) to another aircraft (receiver) in flight. Until today, AAR is only performed in military operations, mainly to extend the range of aircraft with limited fuel capacity [1]. In recent years, civil usage has been analyzed in different research projects. In a first work by Nangia [2] fuel savings and reduced operating costs of up to 40% are predicted. In 2011 multiple European research institutes joined forces in the project ***RE**search on a **CR**uiser **E**nabled **A**ir **T**ransport **E**nvironment* to further investigate civil AAR. Within RECREATE Morscheck [3] conducted a simulation-based analysis for a complete traffic scenario in which he displays benefits regarding the overall fuel consumption of air travel.

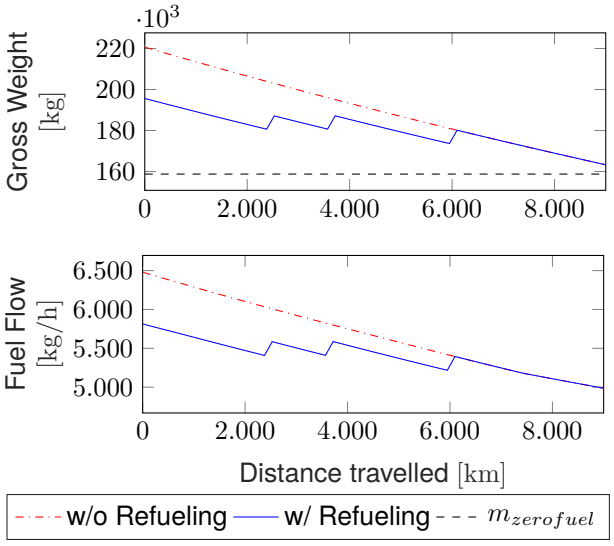

FIG 1. Beneficial effect of AAR on the fuel consumption for a long-haul flight with a wide-body aircraft

The first foreseen effect is the range extension. This allows to operate narrow-body aircrafts with a limited initial range on long-distance flights. Especially for routes with smaller demand this would help to improve the occupancy rate compared to wide-body long-range aircraft. Thus, the fuel consumption per passenger is reduced. Another predicted benefit is the reduction of the gross weight in the early stages of a flight. Since the fuel consumption is directly dependent on the gross weight, it may drop significantly too. Figure 1 qualitatively displays the latter-mentioned idea. It compares a standard flight from Frankfurt to San Francisco without any refuelling and the same mission with multiple in-flight refuellings for the same wide-body aircraft. The simulation is based on the fuel flow data given in the flight crew operating manual of the Boeing B777-200. The refuellings are performed close to Keflavik (Island), Kangerlussuaq (Greenland) and Churchill Airport (Canada) as proposed in [3]. For each refuelling a total fuel transfer of $9000\ \mathrm{kg}$ is assumed. For modern refuelling systems, which are capable of fuel transfer rates of up to $3600\mathrm{kg/min}$ [4], this corresponds to a connection time of $2{,}5$ minutes. Even greater fuel reduction is achievable when AAR is taken into account during conceptional aircraft design as a mean to reduce the maximum takeoff weight as this would allow to reduce the structural mass of future aircrafts.

FIG 2. Example of a tanker equipped for probe-drogue-refuelling [5]

There are two AAR-methods in military aviation. Boom-Refuelling and Probe-Drogue Refuelling (PDR). For Boom-Refuelling, the fuel flows through a rigid pipe which is connected to the aft fuselage of the tanker. The contact is controlled by a designated crew member of the tanker aircraft. Further information on Boom-Refuelling can be found in [1]. For this paper, PDR is considered. For PDR, a drogue is connected to the tanker via a hose and is floating behind the tanker. The receiver aircraft is equipped with a probe. The receiver's pilot directs the probe into the drogue to establish fuel flow [1]. The receiving pilot must precisely control the position of the probe relative to the drogue and its airspeed relative to the tanker, so-called overtake-speed V_{OT}. The latter objective is especially challenging due to the high lag of an aircraft engine, requiring the pilot to apply significant lead regarding airspeed adjustments.
Multiple research projects focused on the automation of AAR. For example, Pachter et al proposed a controller for the position keeption during AAR maneuvers [6] and Williamson et al introduced a concept for

an actively control refuelling drogue [7]. Still, level of automation in real AAR missions is considerably low until today [8]. An extensive analysis of over 250 AAR-related incidents and accidents in [9] concluded that more than 50% of all mishaps were caused by an error of the receiver's pilot, indicating a high pilot workload. In addition, high workload lowers the success rate of AAR maneuvers notably [8]. A significant reduction of the pilot's workload by automation and support systems is therefore mandatory, in order to reliably and safely integrate AAR in civil aviation missions.

Weber and Link [10] introduced two conceptional ideas to integrate the speed brake (SB) in the airspeed control functions to mitigate the effects of the engine's lag. For both concepts, the SB is initially in a partially deflected position. This way, the SB can be used for decelerating as well as accelerating. The first of the two concepts, the so-called Load Factor Augmentation, is designed to reduce the lag in the airspeed response when the pilot is still conventionally controlling it via the thrust lever. After the pilot alters the thrust setting, the SB deflection is automatically adjusted to immediately generate an acceleration corresponding to the new commanded thrust level. The second concept is a fully automated airspeed control law with the SB as its only control variable.

In this paper, we propose flight control law architectures to demonstrate and compare these concepts. These control laws are implemented in a simulation environment and their performance is evaluated by qualified test pilots. The results show improvements regarding the airspeed control, which benefically affects the handling qualities during AAR.

2. SIMULATION MODEL

The SB is used as a primary control surface for the concepts implemented in this paper. Therefore, a simulation model with a good representation of the SB's static and dynamic effects on the overall aircraft dynamics is required. For this purpose, a non-linear model of a high-performance aircraft given by Nguyen in [11] is used, as it already includes an angle-of-attack-dependent depiction of the SB's static effects on the aircraft's aerodynamic coefficients. The model is extended by including the dynamic effects of the SB as well as the correlation between the SB's deflection angle and the resulting aerodynamic coefficients. Both phenomena are modeled based on numerical and experimental investigations of the aerodynamic characteristics of an SB done by Geisbauer in [12]. The basic simulation model as well as the extended SB model will be detailed in the following subsections.

2.1. Basic Simulation Model

In [11] a full non-linear description of the flight dynamics of a high-performance-aircraft can be found. This model is especially suitable for this paper for two reasons. First, a dynamic engine behavior is incorporated, representing the effect of engine lag which is to be addressed in this paper. Second, it also includes the SB as a control surface which is indispensable for the simulation performed in the scope of this paper.

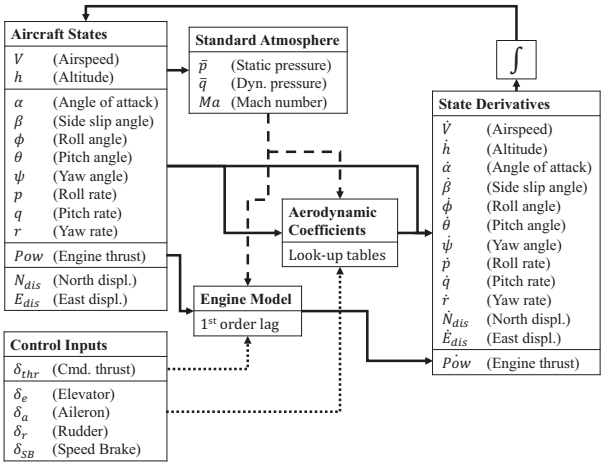

FIG 3. Visualization of the structure of the non-linear simulation model

Figure 3 shows the basic structure of the simulation model. The engine is modeled as a first-order lag system with a time constant of $T_{1,eng} = 1$ s. All other dependencies are described by look-up tables based on the current state of the aircraft. The actuator dynamic of all primary control surfaces is modeled as a first-order lag with a time constant of $T_{1,act} = 0{,}05$ s

2.2. Extended Speed Brake Model

In [11], the SB's influence on the overall dynamics only affects the longitudinal motion as symmetric deflection is assumed. It is modeled by adding corresponding increments to the forward and vertical aerodynamic force coefficient c_x and c_z as well as the pitch moment coefficient c_m. All coefficients are represented in the body frame. In [11], all three SB coefficients are assumed to be solely a function of the angle of attack. The aircraft modeled in [11] uses a different SB concept than a conventional airliner. In contrast to the commonly used spoilers on top of the wing, this aircraft is equipped with so-called decelerons on the inside of the horizontal tailplane. Decelerons consist of one upward and one downward deflecting surface. Figure 4 displays the two different concepts. While the aerodynamic effects of a conventional spoiler might be different, the original setup of [11] is still maintained for consistency within the model. The reference source does not provide an actuator model. As the SB is of similar size and in a similar position as the elevator, it is considered reasonable to use the same actuator model.

FIG 4. Schematic display of different speed brake concepts: conventional spoiler (left) and decelerons (right)

The data in [11] provides the angle-of-attack dependency of the SB's aerodynamic coefficients for full deflection($\delta_{SB} = \delta_{SB,max}$). As the SB will be used in partially deflected positions in the scope of this paper, a first extension of the simulation is done by including a dependency $\Delta c_{i,SB} = f(\delta_{SB})$. In the work of Geisbauer [12] an experimental investigation of this dependency can be found for a conventional spoiler. Approximating decelerons as a pair of two conventional spoilers of which one deflects in the opposite direction, it is considered reasonable to assume similar deflection angle dependencies. While the measurements for the lift and pitch moment coefficient show a linear correlation, the drag coefficient appears to be correlated in a non-linear way to the deflection angle. This dependency is displayed in figure 5.

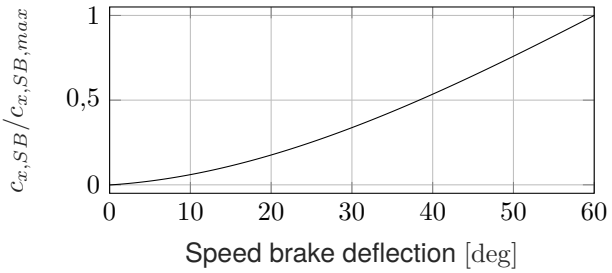

FIG 5. Speed brake drag coefficient as a function of the speed brake deflection angle

The experimental data given in [12] is also used to model the dynamic behavior of the SB' aerodynamic coefficients after a change of the SB deflection as the initial simulation model does not provide any information in this regard. Even though, [12] is referring to conventional spoilers instead of decelerons, the given description of the underlying physical effects allows to consider that decelerons show similar dynamic behavior. The main purpose of an SB is to manipulate the forward sum of forces by increasing the drag of the aircraft. This is predominately caused by a downstream wake space forming after deflecting the SB. According to [12], this is a lag-free phenomenon. In turn, a quasi-stationary effect on the forward aerodynamic coefficient can be assumed. The change in the lift and pitch coefficient is mainly a result of a changed circulation around the wing which is an unsteady process. For this paper, a first-order lag behavior is approximated to model this effect. The time constant is approximated based on data given in [12].

3. CONTROLLER DESIGN

In [10] Weber and Link propose two concepts to mitigate the pilot's workload regarding airspeed control. The first concept, called Load Factor Augmentation (LFA), is intended to support the pilot when the airspeed is conventionally controlled with the thrust lever. This is achieved by compensating the engine lag with the SB. The second concept, called Speed Brake Airspeed Controller (SBAC), is a closed-loop controller that tracks a given reference speed with the SB as its control variable. This paper introduces detailed control architectures which allow to incorporate the two proposed concepts into a flight control system.
For both control laws, the SB is trimmed in a partially deflected position to enable both a decrease and an increase in airspeed. The SB is more effective for higher deflection angles, i.e. the gradient of the drag coefficient becomes larger as shown in figure 5. The drag coefficient reaches 50% of its maximum value for a deflection of $\delta_{SB} \approx 37°$. By setting the initial SB deflection to $\delta_{SB,init} = 40°$, the achievable decrease and increase in drag are of approximately the same absolute value while also accounting for the increased drag gradient at higher deflection angles.

3.1. Load Factor Augmenation

When controlling the airspeed manually, the pilot uses the engine to alter the forward load factor of the aircraft n_x by increasing or decreasing the thrust force. As long as the flight path angle γ is kept constant, this directly results in a proportional change of the velocity gradient $\dot{V}_K$ as shown in the following correlation [13]:

$$n_x = \frac{\dot{V}_K}{g} + \sin(\gamma) \xrightarrow{\gamma=0} \delta n_x \propto \delta \dot{V}_K \tag{1}$$

Due to the engine reaction time, there is a significant time delay before the new stationary load factor is reached after a command. This makes it difficult to precisely control the airspeed, as the pilot must anticipate the aircraft's response. In contrast, a change in the SB's deflection results in a quasi-stationary change of the forward load factor n_x as explained in the previous section. Yet, due to the limited deflection range, the SB itself can not provide sufficient control authority to utilize as the sole control parameter for manual airspeed control.
The idea of the LFA concept is to combine the benefits of both control variables. This is achieved by changing the deflection of the SB after a throttle input to immediately reach the forward load factor that corresponds to the new commanded engine setting. At the same time, the engine starts to adjust. While the engine thrust converges to its new stationary value, the SB is gradually retrieved to its initial position, to maintain a constant load factor. To reduce system complexity, a closed-loop control of the forward load factor by the SB is avoided. Instead, a feed-forward control law (FFC) is implemented which makes use of following characteristic of dynamic systems:

$$G_{LPF} + G_{HPF} = \frac{K}{1+T_1 s} + \frac{K \cdot T_1 s}{1+T_1 s} = K \tag{2}$$

According to this concept, the sum of outputs of a first-order high-pass and a first-order low-pass system with matching time constants to the same input signal is a stationary, proportional signal. In this application,

the engine represents the low-pass. To use the SB as a high-pass system a filter is incorporated making use of its quasi-stationary drag effect. Because of the actuator lag, a perfect first-order high-pass behavior cannot be achieved. Yet it is still expected to improve the airspeed control due to the significantly lower time constant of the actuator compared to the engine. The block diagram of the control law is given in figure 6. To implement the desired FFC, it is necessary to derive an equivalence correlation between the engine and the SB regarding their influence on the resulting change of the forward load factor. This allows to convert a change in the throttle setting $\Delta\delta_{thr}$ into a change of the SB deflection as indicated in figure 6.

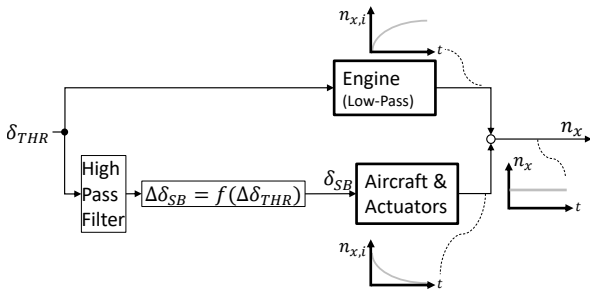

FIG 6. Block diagram of the Load Factor Augmentation control law

To attain the sought-after information, step responses of both engine and SB are simulated. For these simulations, an altitude hold controller is incorporated which ensures a zero path angle. Thus, the property in equation 1 can be utilized to determine the load factor from the acceleration. Based on the step responses, SB deflection changes and engine setting changes with the same resulting acceleration, i.e. the same change of the forward load factor, can be matched to form one point of a characteristic curve.

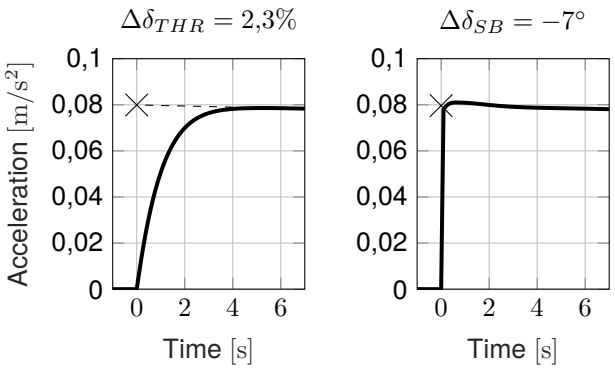

FIG 7. Step responses of airspeed gradient to engine and speed brake inputs showing the concept of load factor equivalency by matching the extrapolated constant acceleration (cross)

Figure 7 shows an example match. As the characteristic curve shall correlate the steady-state values, the engine acceleration is extrapolated to the time of step as indicated by the dashed line in figure 7 left.
The resulting characteristic line is displayed in figure 8. It indicates that there are rather restrictive limits to

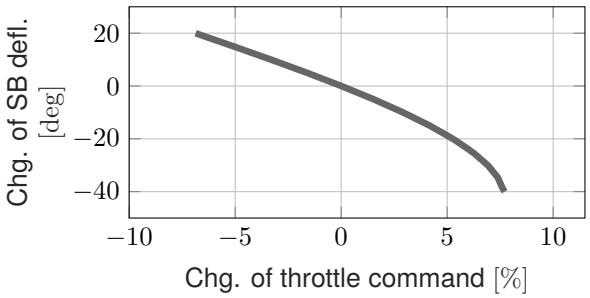

FIG 8. Characteristic Curve representing the equivalence correlation of engine and speed brake

the LFA. When a pilot's command exceeds these limits, the SB will reach its deflection limit. As a consequence, the engine lag cannot be fully compensated anymore. This issue is further depicted by figure 9. It compares a thrust command within the achievable range to one outside of it. Once the SB is fully retracted, it can no longer compensate for the engine lag. In turn, the acceleration of the aircraft is mainly affected by the engine dynamics again. This represents a non-linearity in the control law. To avoid undesirable pilot-interactions with this non-linearity, cockpit indications are necessary to ensure situation awareness. This is further discussed in section 4.

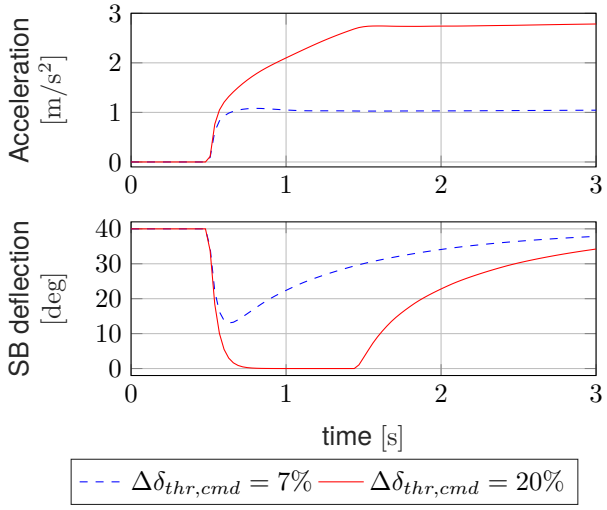

FIG 9. Effect of speed brake deflection limits on the performance of the LFA control law

3.2. Speed Brake Airspeed Controller

The aim of the SBAC is to provide a closed-loop controller to track a reference airspeed. In contrast to conventional laws, it uses the SB instead of the engine as its control parameter. As mentioned before, the SB is partially deflected initially which allows to control the airspeed in both directions. Due to the resulting additional drag in trimmed flight and the deflection limits of the SB, this control law is not suitable for long-term maneuvers or maneuvers with large airspeed gradients. As neither applies to AAR, the SBAC is seen as beneficial for this application. The engine thrust

is kept constant allowing to use single-input-single-output control design methods.

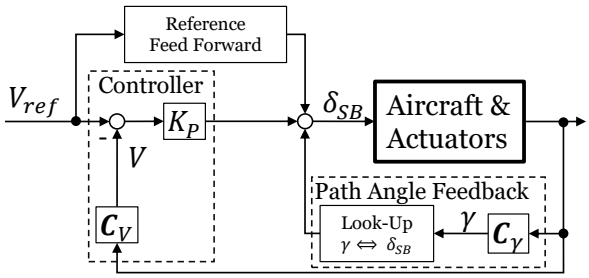

FIG 10. Block diagram of the Speed Brake Airspeed Controller

Figure 10 shows the block diagram of the control law. Besides the closed-loop controller, it features two additional functions. The first is a reference feed forward. It is intended to improve the performance when the reference airspeed is changed. The second function is a non-linear path angle feedback to avoid stationary tracking errors due to path angle deviations. Each function is described in detail in this section. The control law can be given as:

$$\delta_{SB,cmd} = \delta_{SB,ctrl} + \delta_{SB,\gamma} + \delta_{SB,ffc} \tag{3}$$

Closed loop controller

The controller itself is implemented as a proportional gain controller. Unlike other standard controllers, it does not include an I- or D-component. While the latter ensures a faster reaction to a change of the reference airspeed V_{ref}, it also causes an undesirable, higher reactivity to changes in the measured airspeed, i.e. to turbulence and measurement noise. As the reference feed forward already accounts for changes of V_{ref} a D-component can be evaded to avoid its mentioned disadvantages. The controller features no I-component, as this results in a slower controller performance and could lead to wind-up problems. The downside of avoiding an I-component is the potential for a stationary tracking error. This is not a problem for horizontal flight as there is an integrating behavior within the plant for $\gamma = 0$ as shown in equation 1. To avoid stationary tracking errors for nonzero path angles the path angle feedback is included. The SB deflection is calculated accordingly as:

$$\delta_{SB,ctrl} = K_p \cdot \Delta V_k \tag{4}$$

The upper boundary for the controller gain $K_{p,max}$ results from the gain margin with respect to the critical controller gain for neutral stability $K_{p,crit}$ as required by MIL-DTL-9490 [14]. To achieve a fast tracking behavior, the gain is maximized within this upper boundary as indicated by figure 11. Depending on the location of the phugoid poles, this may lead to an undesirable oscillating system response, which would add another upper boundary to the controller gain. This is not the case for the model used in this paper.

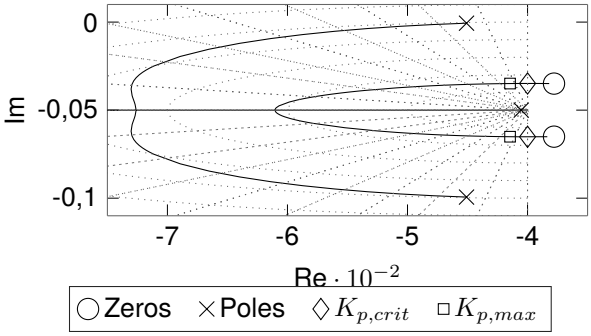

FIG 11. Root locus to determine controller gain K_p

Non-linear path angle feedback

For a constant reference airspeed the control law of equation 3 can be incorporated in the definition of the forward load factor given by equation 1 as follows. f_{n_x} represents the effect of a change in the SB deflection on the forward load factor derived from step responses as indicated in figure 7.

$$n_x = f_{nx}\left(\delta_{SB,ctrl} + \delta_{SB,\gamma}\right) = \frac{\dot{V}_K}{g} + \sin(\gamma) \tag{5}$$

By applying linear approximation regarding the SB-load factor correlation f_{n_x} for once. equation 5 can be approximated and rearranged as:

$$\frac{\dot{V}_K}{g} = f_{nx}\left(\delta_{SB,ctrl}\right) + f_{nx}\left(\delta_{SB,\gamma}\right) - \sin(\gamma) \tag{6}$$

The sought-after path angle feedback definition is derived from demanding the last two terms to cancel each other. In this way, the SB deflection commanded by the closed-loop controller $\delta_{SB,ctrl}$ is directly influencing the acceleration of the total velocity, achieving integrating characteristics regarding the airspeed as desired. Therefore the SB deflection commanded by the non-linear path angle feedback is determined as:

$$\delta_{SB,\gamma} = f_{nx}^{-1}\left[\sin(\gamma)\right] \tag{7}$$

The inverse function is implemented based on the step input data of the acceleration the changes in of the SB deflection shown in figure 7 right.
Figure 12 displays the effect of this function for a maneuver with a constant rate of climb. Without the path angle feedback, a stationary control error is present whereas the aircraft maintains the reference airspeed during the stationary phase of the maneuver with the function active. As the SB has a limited deflection range, it can only compensate the path angle to a certain level. In the case of the aircraft model used for this paper, the achievable path angle range appeared to be sufficient for AAR maneuvers. Otherwise, a more

complex control law which also includes the engine as a control parameter would be necessary.

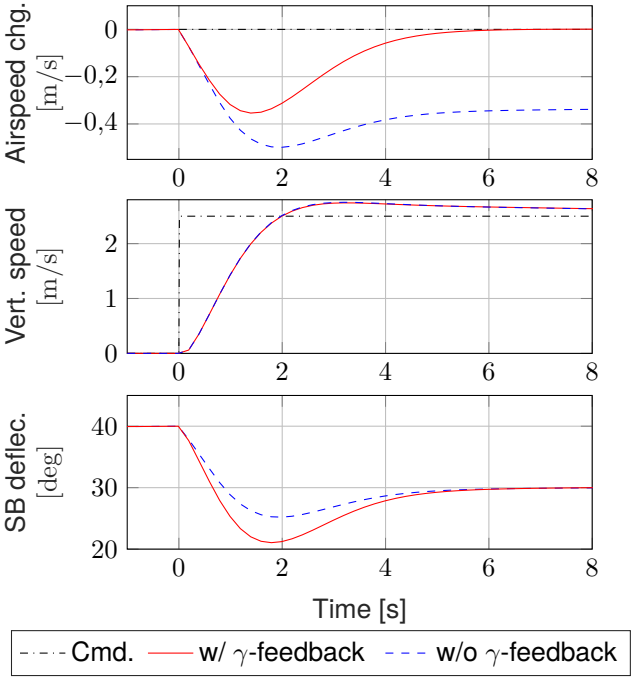

FIG 12. Effect of path angle feedback for a simulated maneuver with a constant vertical speed

Reference feed forward

The reference FFC is added to improve the performance of the controller after a change to the reference airspeed. Would the SB be only driven by the control error, it would gradually approach its initial position once the control error gets smaller. As the SB does not make use of its full range, this results in a longer time to reach the new reference than needed. The reference FFC mitigates this effect.

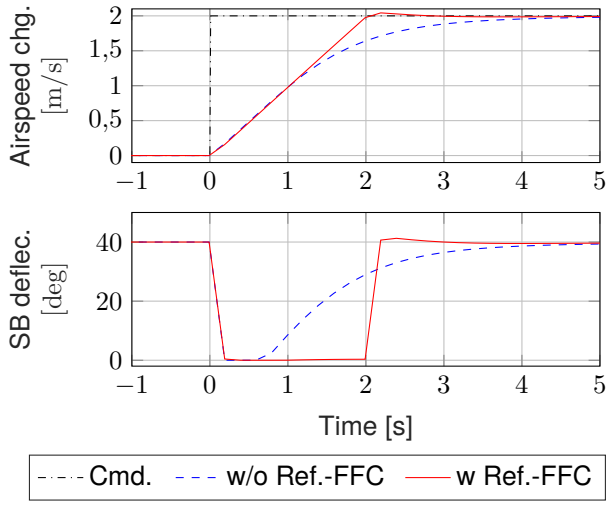

FIG 13. Effect of reference feed forward sub-function

The idea of this function is to fully deflect or retrieve the SB for a given time period so that the new airspeed command is established with a constant gradient as illustrated in figure 13. As this figure highlights, the new airspeed is reached about $1{,}5$ s faster than without this function. This is achieved by a logic which detects a change of the reference airspeed V_{ref} and then commands a full deflection or retraction of the SB. The deflection time t_{ffc} is calculated based on the step height of the reference airspeed ΔV_{ref} and the maximum acceleration/deceleration attainable by means of the SB itself $|\dot{V}_{SB}|_{max}$:

$$t_{ffc} = \frac{\Delta V_{ref}}{|\dot{V}_{SB}|_{max}} \tag{8}$$

4. SIMULATION TEST CAMPAIGN

A simulation test campaign with qualified, AAR-experienced test pilots was conducted to further evaluate the designed control laws. This campaign was done in cooperation with the German Aerospace Center in Manching. A fixed-base simulator with a sidestick and a thrust lever as control elements was used. For visualization, a dynamic vector-graphic program was used. It schematically depicted the environment by displaying two-dimensional elementary shapes like lines, polygons, and ellipses. An example of the visualization is given in figure 14.

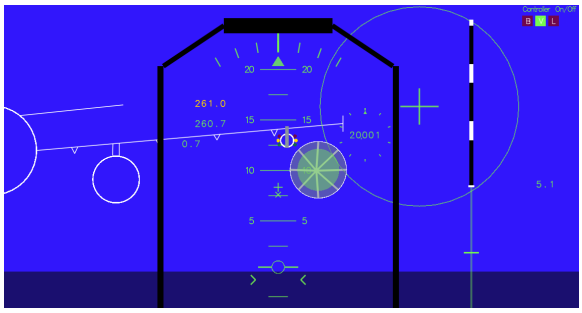

FIG 14. Exemplary presentation of the visualization used in the test campaign

The primary flight information was provided in a schematic head-up display (HUD). Besides indications of airspeed, altitude, and attitude, the visualization also included a flight path indicator and a specific excess power (SEP) marker. Together, they provided a perception level of the airspeed dynamics comparable to such in current generation commercial airplanes. The position of the probe was indicated by a large horizontal cross to the right of the HUD. The drogue was depicted as a circular shape that changed in size based on the distance of the receiver to it. At the point of contact, the drogue had the same diameter as the circle around the probe's cross. This was supposed to give the pilot an impression of the relative distance to the drogue, as this is otherwise difficult to perceive in a two-dimensional visualization. For the LFA, the SEP-indication was extended to highlight the limited operational range mentioned in section 3.1. For the SBAC, two buttons at the backside of the sidestick were used to change the commanded airspeed by increments of $0{,}5$ kt.

The test campaign was split into two segments. In the first phase, the pilots were asked to fulfill airspeed tracking tasks. In the second phase, AAR maneuvers were performed to evaluate the influence of the designed control laws on AAR. In each phase, the tests were performed with the regular engine-only airspeed control as a baseline and with both control laws introduced in this paper. All tests were executed at an airspeed of $V = 260\ \mathrm{kt}$ in flight level FL200.
The Cooper-Harper-Rating-scale (CHR) was used for all tests as a metric to evaluate the pilot's handling quality perception. Details on the CHR can be found in [15]. Further, additional data-based parameters specifically defined for each task are regarded. These are introduced in the corresponding sections.

4.1. Evaluation of Airspeed Tracking Performance

The first phase of the test is intended to gain information about the control law's general influence on airspeed control. To do so, the pilots are asked to perform changes in airspeed of $\pm 3\ \mathrm{kt}$, which is similar to the range of airspeed deviations commanded during AAR maneuvers [16]. Meanwhile, the pilot is supposed to maintain a constant altitude. The first performance parameter is the CHR. The CHR accounts for the necessary pilot compensation as well as the task performance. For the latter, measurable objectives, which define desirable and adequate performance, must be given. They are determined based on statements given by AAR-experienced test pilots as well as available information regarding necessary speed accuracy during AAR as given in [16] and [17]. The values are states in table 1.

	Capture		Maintenance	
	des.	adeq.	des.	adeq.
Airspeed	1,0 kts	2,0 kts	0,5 kts	1,0 kts
Altitude	25 ft	50 ft	12,5 ft	25 ft

TAB 1. Performance Objective for Cooper-Harper rating for airspeed tracking tasks

Besides the CHR, the capture time t_{cap}, the number of control reversals n_{cr}, and the time-averaged altitude error $e_{h,\mathrm{avg}}$ are used for evaluation. The capture time is the time from the first control input until the airspeed is established within a range of $\pm 0{,}5\ \mathrm{kt}$ around the target airspeed. The number of control reversals is a way to evaluate the pilot compensation. In this paper, a control reversal is understood as a control input's crossing of its initial/trim value. This indicates a counteraction of the pilot against a previous input. As the pilot is not controlling the airspeed himself with the SBAC, the number of control reversals is not determined for said control law. The time-averaged altitude error is analyzing how much the pilot can focus on the secondary task of maintaining the altitude. It is defined as:

$$e_{h,avg} = \frac{\int_{t_s}^{t_e} |h(t) - h_{init}| dt}{t_e - t_s} \tag{9}$$

where h is the altitude of the aircraft, t_s is the start time of the maneuver and t_e the end time. To determine the number of control reversals and time-averaged altitude error a time-span two seconds beyond the capture time is regarded to account for corrections performed to stay within the accuracy limits. Figure 15 displays the metrics used to evaluate the airspeed tracking performance.

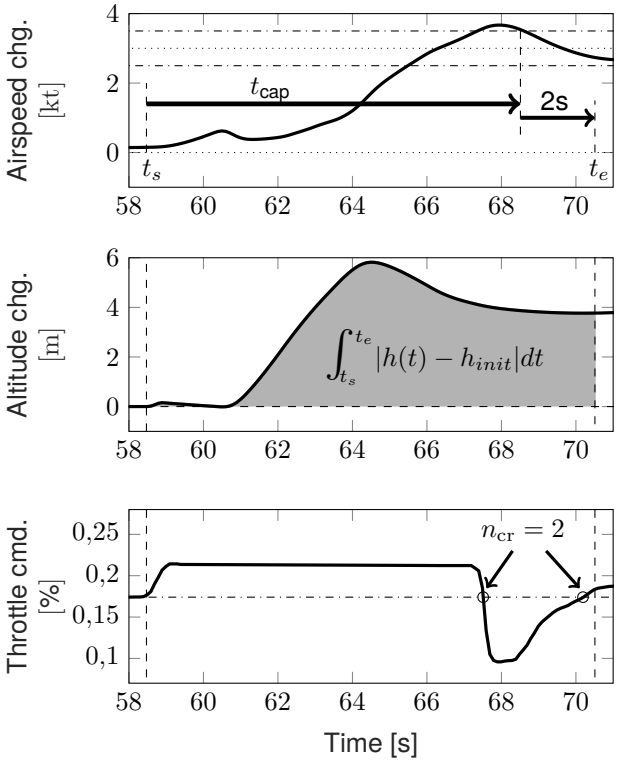

FIG 15. Exemplary presentation of the data-based metrics used for performance evaluation

Especially the capture time and the number of control reversals are dependent on the pilot gain, i.e. the aggressiveness applied by the pilot. As this is an individual parameter, only values obtained from flight tests with the same test pilot can be compared. Each pilot performed the airspeed capture task various times in both directions. The average values of these parameters for each pilot with each control law as well as the CHR assigned by the pilots are given in tables 2 to 5.

	Engine only	LFA	SBAC
Test Pilot 1	3,57 s	2,02 s	2,89 s
Test Pilot 2	8,11 s	6,01 s	2,74 s
Test Pilot 3	7,81 s	3,70 s	2,84 s

TAB 2. Average values for capture time for each test pilot for airspeed capture tasks

	Engine only	LFA	SBAC
Test Pilot 1	0,174 m	0,137 m	0,154 m
Test Pilot 2	1,183 m	0,967 m	0,139 m
Test Pilot 3	1,293 m	0,195 m	0,348 m

TAB 3. Average values for time-averaged altitude error for each test pilot for airspeed capture tasks

	Engine only	LFA
Test Pilot 1	1,80	0,40
Test Pilot 2	3,00	1,40
Test Pilot 3	2,00	0,75

TAB 4. Average values for number of control reversals for each test pilot for airspeed capture tasks

	Engine only	LFA	SBAC
Test Pilot 1	3	2	1
Test Pilot 2	3	1	1
Test Pilot 3	4	2	1

TAB 5. Cooper-Harper-ratings given by each test pilot for airspeed capture tasks

All parameters indicate an improved airspeed control with both control laws compared to the conventional (engine only) control law. The capture time in table 3 decreased significantly for both control concepts. While it is highly dependent on the pilot with the conventional control and LFA, it is almost the same for all three pilots with the SBAC. This is to be expected as the pilot is not in the loop regarding airspeed control and the airspeed gradient is fixed due to the SB's deflection limits. Therefore, the pilot gain is not a factor. Interestingly, despite assigning a better CHR for the SBAC compared to the LFA, the time-averaged altitude error in table 3 indicates better performance with the LFA for pilots 1 and 3. One reason for this could be that the reduction to only one task objective controlled by themselves made the pilots be more relaxed. In turn, this might have led to a higher tolerance regarding altitude deviations.
All analyzed parameters indicate that both control laws designed in this paper improve the airspeed control performance and reduce the necessary pilot compensation. Yet, for a stronger statement further tests and data are need to build up a statistical tendency.

4.2. Evaluation of Air-to-Air-Refuelling Performance

After successfully testing the control laws regarding the airspeed tracking performance, the second test phase is intended to evaluate their influence on the overall performance during AAR maneuvers. Due to the limited capabilities of the simulation visualization, the test only included the transition from the so-called pre-contact to the contact position. The pre-contact position is a position up to $6\ \mathrm{m}$ behind the drogue [17].

In a real AAR maneuver the receiver pilot first establishes and maintains this position without any overtake speed before being cleared to move into the contact position and connect to the drogue. As this transition requires the highest accuracy regarding position and airspeed control, it is considered reasonable to disregard the other phases. In this test campaign, the simulation started at a fixed distance from the drogue. The vertical and lateral starting positions are altered for each repetition with a standard deviation of one drogue diameter. The objective for the pilot is to establish an overtake speed within the range of $1{,}5\ \mathrm{kt}$ to $4{,}0\ \mathrm{kt}$ and to connect to the drogue as centered as possible. Table 6 states the performance objectives for the CHR rating based on [18]. The green-shaded part of the drogue in figure 14 shows the desired contact area.

	desired	adequate
Contact	half drogue radius	full drogue radius
Airspeed	V_{OT}-range	range $\pm 1\ \mathrm{kts}$

TAB 6. Performance Objective for Cooper-Harper rating for air-to-air-refueling tasks

Besides CHR, the contact precision index (CPI) and the contact success rate (CSR) are considered for performance evaluation. Regarding the contact point, it can be generally said that the more off-center a contact, the higher the chance that contact is unsuccessful. This is due to a tilting moment around the drogue's anchor point initiated by the probe's impulse. Therefore, the contact should be established as centered as possible but at least within the inner 75% of the drogue radius r_{dr} to be considered successful [10]. Based on this assumption the CPI is defined as:

$$\text{CPI} = \frac{\sqrt{(y_{dr} - y_{pr})^2 + (z_{dr} - z_{pr})^2}}{0{,}75 \cdot r_{dr}} \tag{10}$$

y_{dr} and z_{dr} are the lateral and vertical position of the drogue and y_{pr} and z_{pr} are the respective values of the probe in the moment of contact. A CPI between 0 and 1 corresponds to a contact within the required part of the drogue. CSR is defined as the fraction of all attempts in which the pilot achieves a CPI below 1 while being within the required range for the overtake speed. The test is repeated at least ten times by each pilot for each control law. The order in which the control laws are tested is altered to avoid a learning curve bias in the overall data. To flatten a potential learning curve, the pilots also performed about five simulations without data recording to get used to the visualization. Based on all recorded repetitions, the CSR is determined, and the average value as well as the standard deviation (SD) of the CPI is calculated for each pilot. The AAR-related tests were only conducted with test pilots 2 and 3. The performance parameters are displayed in tables 7 to 9.

	Engine only	LFA	SBAC
Test Pilot 2	8	7	7
Test Pilot 3	8	6	7

TAB 7. Cooper-Harper-ratings given by each test pilot for air-to-air-refueling tasks

	Engine only	LFA	SBAC
Test Pilot 2	27,3%	10,0%	50,0%
Test Pilot 3	38,9%	30,8%	63,6%

TAB 8. Contact success rate given by each test pilot for air-to-air-refueling tasks

The CHR indicates a poor level of handling qualities as both pilots assigned ratings associated with level 3 handling qualities. The pilots stated that especially the perception and control of their relative vertical and lateral position to the drogue felt inadequate. The reason for this cannot be determined unequivocally. Two potential aggravating factors are the simulation model which might not be optimized for simulations of AAR and the visualization setup, which is missing some important visual references like the fuel hose. In turn, airspeed control is only a subordinate factor making it difficult to evaluate the influence of the alternate airspeed control laws. Still, the control laws slightly improve the CHR as shown in table 7.

Regarding the data-based criteria, the SBAC shows significant improvements as the CSR given in table 8 is almost doubled for both test pilots. As table 9 shows, the CPI decreased noticeably for pilot 2 and slightly for pilot 3. Yet, for pilot 3 this change is well within a range of statistical uncertainties given the small number of samples and the rather high standard deviations. In contrast to the CHR, the data-based parameter indicates a degraded performance with the LFA activated. In case of the CPI, statistical effects can not be ruled out as a reason, as the standard deviations are high for both the conventional airspeed control and the LFA.

To identify potential causes of the decreased CSR the failed approaches are analyzed in detail. It is discovered that for conventional airspeed control both test pilots always met the speed requirement when the position was within the inner 75% of the drogue. I.e. the main contributor to the CSR is the position tracking. In contrast, for the LFA both pilots had numerous cases in which they were slower than the required overtake speed in the moment of contact despite meeting the position requirements. Mostly, this happened because the overtake speed fell below the lower limit of V_{OT} within the last second before contact, as indicated by figure 16. In real AAR-maneuvers, a pilot must reduce the overtake speed to zero as soon as contact is established. This requires retrieving the throttle slightly before contact to compensate for the engine lag. It is likely that this behavior was subconsciously applied causing the

		Engine only	LFA	SBAC
Test Pilot 2	*Avg.*	1,72	1,75	1,20
	SD	1,12	1,09	0,80
Test Pilot 3	Avg.	1,05	1,17	1,00
	SD	0,80	0,76	,38

TAB 9. Contact precision index given by each test pilot for air-to-air-refueling tasks

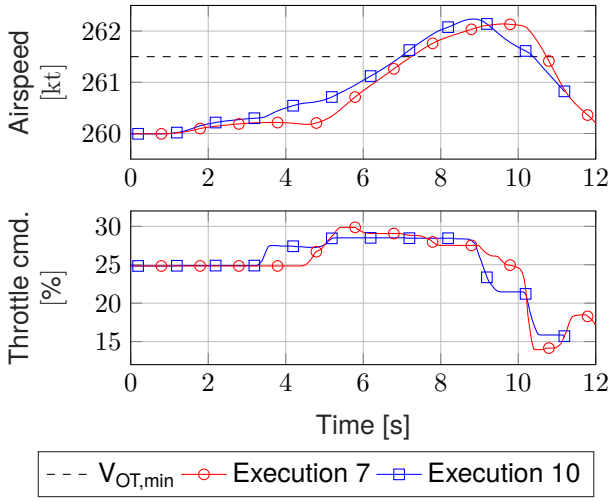

FIG 16. Airspeed data for two cases in which the speed requirement was missed due to overcompensation with the load factor augmentation active

overtake speed to reduce to early as the LFA compensates for the engine lag already. It is assumed that this problem can be mitigated when a pilot becomes more experienced with the LFA.

5. CONCLUSION

In this paper, two control law modifications are presented that automatically integrate the speed brake into the control architecture to allow for fast and precise airspeed control. Such control laws are seen as potential enabling technologies for civil air-to-air-refuelling. In a first approach, the speed brake is used to compensate for the engine lag when the thrust is manually commanded by the pilot. The second modification is a closed-loop tracking controller which uses the speed brake instead of the engine for airspeed tracking to achieve a faster system response. This paper defines performance metrics to test airspeed control law modifications. In a simulation test campaign, both control laws show beneficial effects when being tested in isolated airspeed tracking tasks. This is indicated by improvements in the Cooper-Harper-rating as well as enhancements in data based performance metrics. This paper also investigates the effects of the control laws on the pilot workload in high-precision flight tasks like air-to-air-refuelling. The findings of this test have a limited conclusiveness the primary challenge for the pilots in the baseline test was position control rather than airspeed control. Still

slight improvements regarding the Cooper-Harper-ratings were achieved with the control laws in place. To better evaluate the potential of the designed control laws, future research could focus on testing them in a better-suited simulation environment with a more realistic visualization setup and a more sophisticated flight mechanical model.

ACKNOWLEDGMENTS

This paper is based on the findings of a master's thesis, which was developed in cooperation with the Institute for Flight Systems of the German Aerospace Center in Manching. The intellectual and technical support provided by Dr. Ina Rüdinger and her team is highly appreciated.

Contact address:

h.wilke@tu-berlin.de

References

[1] Richard K. Smith. *Seventy-Five Years of Inflight Refueling*. Air Force History and Museums Program, 1998. ISBN: 978-1500520090.

[2] Rajendar K. Nangia. Operations and aircraft design towards greener civil aviation using air-to-air refueling. *THE AERONAUTICAL JOURNAL*, 110(1113), November 2006. DOI: 10.1017/S0001924000001585.

[3] Fabian Morscheck. Analyses on a civil air to air refueling network in a traffic simulation. *29th Congress of the International Council of the Aeronautical Scienes*, September 2014.

[4] Airbus (publ.). Airbus a330 mrtt - technical. 2023. https://www.airbus.com/en/products-services/defence/military-aircraft/a330-mrtt.

[5] Khalem Chapman. Raf vip voyager resumes tanker operations. June 2020. https://www.key.aero/article/rafs-vip-voyager-resumes-tanker-operations.

[6] Meir N. Pachter et al. Development of an air-to-air refueling automatic flight control system using quantitative feedback theory. *International Journal of Robust and Nonlinear Control*, 7, November 1997. DOI: 10.1002/sici-1099-1239.

[7] Walton R. Williamson et al. Controllable drogue for automated aerial refueling. *Journal of Aircraft*, 47:515 – 527, April 2010. DOI: 10.2514/1.44758.

[8] Tevfik Erkin et al. Vision-based autonomous aerial refueling. *AIAA SciTech Forum*, January 2022. DOI: 10.2514/6.2022-1384.

[9] Marvin L. Thomas. *Analysis of the causes of inflight refueling mishaps with the KC-135*. Air Force Institute of Technology, 1989.

[10] Philipp Weber and Philipp Link. Simulator testing of semi-automated control concepts for the receiver aircraft during air-to-air-refueling with probe-drogue-systems. *SFTE European Chapter Symposium*, 2002.

[11] Luat T. Nguyen et al. *Simulator Study of Stall/PostStall Characteristics of a Fighter Airplane With Relaxed Longitudinal Static Stability*. National Aeronautics and Space Administration, 1979.

[12] Sven Geisbauer. Numerical simulation and validation of aerodynamics of static and dynamic spoilers. *Journal of Aircraft*, 58:1–17, July 2021. DOI: 10.2514/1.C036145.

[13] Karoline Schreiter et al. nxcontrol: Konzept zur Vorgabereglung für die Längsbeschleunigung des Flugzeugs. *Deutscher Luft- und Raumfahrtkongress*, September 2013.

[14] United States Department of Defence. Flight Control Systems - Design, Installation and Test of Piloted Aircraft General Specification. Standard, Apr. 2019. MIL-DTL-9490.

[15] George E. Cooper and Robert P. Harper. *The Use of Pilot Rating in the Evaluation of Aircraft Handling Qualities*. Advisory Group For Aerospace Research and Development, 1969.

[16] Peter Thomas et al. Advances in air to air refueling. *Progress in Aerospace Sciences*, 71, November 2014. DOI: 10.1016/j.paerosci.2014.07.001.

[17] Ryan Ryan Dibley and Michael Allen. *Autonomous Airborne Refueling Demonstration, Phase I Flight-Test Results*. National Aeronautics and Space Administration, 2007.

[18] Robert Tipton et al. *Aerial Refueling Test Methods*. Aerial Refueling Systems Advisory Group, 2015.